Nile Journal of Communication & Computer Science

Volume 9, June 2025

Journal Webpage: https://njccs.journals.ekb.eg

An Effective Bladder Cancer Diagnosis Strategy (BCDS) based on Deep learning and Artificial intelligence techniques

Rana A. El- Atier[1,*], M. S. Saraya[1], Ahmed I. Saleh[1], and Asmaa H. Rabie[1]

[1] Computers and control Dept. Faculty of engineering Department, Faculty of engineering, Mansoura University, Mansoura 35516, Egypt

Corresponding Author: Rana Ahmed El-Atier. Email: eng.r.ahmed2288@gmail.com

Abstract

Bladder cancer, one of the most common tumors of the urinary system, requires an early and correct diagnosis to optimize survival and treatment results. This research introduces the Bladder Cancer Diagnosis Strategy (BCDS), a two-phase methodology that uses AI-powered image processing to improve bladder cancer detection. In the Pre-Processing Phase (PP), picture data is balanced and enhanced to guarantee variety, followed by feature extraction using pre-trained deep learning models like GoogleNet, DenseNet, and AlexNet. These models are chosen based on their complementing architectural qualities, which ensure a balance of performance and computational economy. The retrieved features are refined using Leopard Seal Optimization (LSO) for feature selection and the Interquartile Range (IQR) approach for outlier removal. During the Bladder Cancer Diagnosis Phase (BDP), the K-Nearest Neighbors (KNN) classifier is optimized using Grid Search cross-validation, which investigates alternative combinations of hyper parameters (such as the number of neighbors and distance measure) to maximize classification accuracy. A comparison study using ResNet-50 was also done, which revealed that the suggested technique performed similarly or slightly better at a lower computational cost. The experimental findings show that the suggested BCDS has an accuracy of 97%, precision of 94%, recall of 95%, and an F1-score of 96%, indicating that it is effective for clinical use. Future research will focus on increasing dataset variety, implementing real-time diagnostic capabilities, and investigating advanced AI models to improve bladder cancer diagnosis.

Keywords: Artificial intelligence, Deep Learning, Bladder Cancer, Classification, Diagnosis.

1. Introduction

One of the most prevalent cancers affecting the urinary system is bladder cancer, which is defined by the unchecked proliferation of aberrant cells in the bladder lining. [1] Males are more likely than females to experience it, and older persons are more likely to do so. The main risk factors are a history of radiation therapy or chemotherapy, smoking, exposure to industrial chemicals, and persistent bladder infections.

The most prevalent kind of the illness is urothelial carcinoma (transitional cell carcinoma), which is divided into many categories according to histological characteristics. Adenocarcinoma and squamous cell carcinoma are two forms that are less common. [2] Frequent urination, dysuria (painful urination), painless hematuria (blood in pee), and, in more advanced instances, pelvic discomfort or weight loss are the usual

symptoms of bladder cancer. The prognosis is greatly improved by early diagnosis and therapy. Urine cytology, cystoscopy, and imaging procedures like CT urograms are examples of diagnostic approaches. [3] Depending on the stage of the malignancy, treatment options might include intravesical therapy, chemotherapy, radiation therapy, transurethral resection of bladder tumor (TURBT), or radical cystectomy in more advanced instances.

The medical industry has undergone a revolution thanks to AI and machine learning (ML), which have improved the precision, effectiveness, and individualization of illness diagnosis and treatment. [4] These tools use enormous volumes of medical data, such as genetic profiles, imaging, and clinical records, to find trends that help medical practitioners make decisions. AI and ML have demonstrated significant promise in the early detection, diagnosis, and tailored treatment of bladder cancer. AI-driven image recognition systems increase the precision of bladder tumor detection using imaging methods like magnetic resonance imaging (MRI) and computed tomography (CT). Furthermore, bladder cancer biomarkers are found using ML algorithms that examine blood and urine samples, allowing for prompt detection and treatment [5].

Despite these developments, bladder cancer remains a major worldwide health problem, as seen in Figure 1 [13]. Accurate and prompt diagnosis is critical for increasing survival rates and facilitating successful treatment. However, classic diagnostic procedures including cystoscopy, urine cytology, and histopathological examination have significant disadvantages, including subjectivity, invasiveness, high cost, and inter-observer variability [10]. Furthermore, these approaches frequently lack the sensitivity and specificity needed for early-stage detection, which can result in delayed diagnosis and poor treatment results.

In recent years, AI and machine learning have emerged as viable solutions to these difficulties. Deep learning models, particularly Convolutional Neural Networks (CNNs), have proven to be highly accurate in medical image processing, tumor localization, and malignancy classification. These models may learn complex characteristics from a variety of imaging modalities, including histological slides, multipara metric MRI (mpMRI), and cryptoscopic images [11]. They have also been used to automate tumor segmentation, grading, and recurrence prediction, which helps clinical decision-making and reduces diagnostic mistakes.

Nonetheless, numerous hurdles remain in using AI technologies for bladder cancer detection. Access to big, well-annotated datasets is critical for constructing strong AI models, but these datasets are frequently limited by privacy concerns and data-sharing restrictions [12]. Furthermore, further research is needed to improve AI systems' interpretability and generalizability across various demographics and imaging settings. Regulatory approval and comprehensive clinical validation are also required to assure its dependability and safety in real-world settings.

More precise diagnosis, better treatment planning, and higher survival rates for individuals with bladder cancer are all anticipated as AI and ML continue to develop and are incorporated into healthcare. However, for broad use, issues including clinical validation, algorithm openness, and data privacy need to be resolved. [6]

KNN is a popular machine learning algorithm in medical diagnosis and illness treatment because of its ease of use, efficacy, and capacity to categorize complicated datasets [7]. KNN functions as an instance-based, non-parametric learning technique, which makes it appropriate for genetic profiling, illness prediction, and pattern identification in medical imaging.

Pre-trained convolutional neural networks (CNNs) can extract relevant characteristics from complicated medical pictures like X-rays, CT scans, and MRI scans, so they have become indispensable in medical image

analysis and illness detection. Large-scale datasets are used to train these networks initially, and transfer learning may then be used to tailor them for particular medicinal uses. [8] Pre-trained CNNs help clinicians identify illnesses like cancer, pneumonia, and neurological problems with high accuracy by identifying complex patterns and abnormalities in medical pictures. Because of their capacity to automate feature extraction, less manual analysis is required, which speeds up and improves the efficiency of the diagnostic procedure. Additionally, by enhancing early illness diagnosis, these models contribute to enhance patient care and treatment results.

The hunting techniques of leopard seals served as the inspiration for the metaheuristic algorithm known as Leopard Seal Optimization (LSO)[29]. It was created to address challenging optimization issues in a number of fields, including the interpretation of medical images [9]. Because of its reputation for effectively navigating search spaces and avoiding local optima, LSO is especially useful for identifying the most pertinent characteristics in huge medical datasets. LSO is essential to feature selection in medical image processing since it helps to improve the accuracy of illness categorization by selecting the most distinguishing features from images like CT and MRI scans. In contrast to other optimization algorithms like Tuna Swarm Optimization (TSO) and Pelican Optimization Algorithm (POA), research has demonstrated that employing LSO for feature selection has enhanced diagnostic model performance.

In this paper BCDS has been introduced to diagnose bladder cancer. BCDS divides into two phases. Pre-Processing Phase (PP) and the Bladder Cancer Diagnosing Phase (BDP) to obtain accurate result. The first phase consists three phases feature extraction, feature selection, and outlier rejection. In feature extraction phase uses pre-trained models and choose the best result of them then feature extraction phase uses LSO. Finally reject outliers uses IQR. the output of this phase enter to classification phase to diagnose the case BCDS provided the maximum accuracy, precision, recall, micro average recall and precision, macro average recall and precision, and F1-measure and also it provided the minimum timing of execution and error.

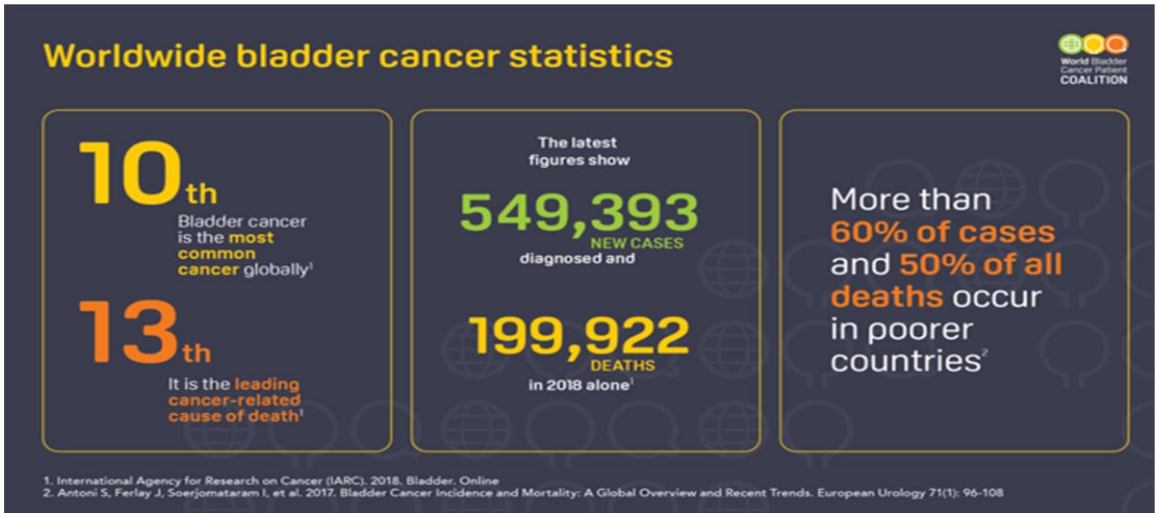

Fig 1. Worldwide bladder cancer statistics

The remainder of the paper is organized as follows: Section 2 defines the problem. Section 3 reviews related work on disease diagnosis using Deep Learning and Artificial Intelligence (AI). Section 4 outlines the proposed Bladder Cancer Diagnosis Strategy (BCDS). Section 5 presents the experimental results. Finally, Section 6 concludes the paper and discusses future work

2. Related work

In [14], an immune-based prognostic learning model (IBPLM) was developed to classify bladder cancer (BCa) patients based on the tumor immune microenvironment (TIME). The IBPLM framework consists of two stages: first, ten machine learning algorithms were integrated to construct the immune signature, identifying key prognostic features. In the second stage, a deep learning technique was employed to detect the IBPLM subtype directly from pathological images, improving automated diagnosis. The results demonstrated that IBPLM serves as an independent prognostic factor for overall survival (OS) and effectively predicts response to immune checkpoint inhibitors (ICI) and chemotherapy. However, despite its promising performance, the model requires further clinical validation and is computationally demanding due to the complexity of the integrated algorithms.

In [15], an AI-driven bladder cancer diagnosis model (AIBCM) was introduced to get the accuracy and consistency of BCa diagnosis by addressing the limitations of operator-dependent diagnostic tools. The AIBCM framework consists of two stages: in the first stage, AI was applied to improve detection and classification across three key diagnostic areas cystoscopy, clinical tumor (cT) staging, and pathological diagnosis. In the second stage, its role in precision medicine was analyzed, demonstrating its potential to refine molecular characterization and guide patient-specific treatment strategies. Although AIBCM showed promising results, further large-scale prospective studies are required to validate its effectiveness and integration into routine clinical practice.

In [16], an AI-assisted urinary cytology model (AIUC) was developed to enhance the diagnostic accuracy and efficiency of bladder cancer detection using urine cytology slides and whole-slide images (WSIs). The AIUC framework consisted of two stages: in the first stage, a cytopathologist and two cytotechnologists reviewed urine cytology samples using three diagnostic modalities—traditional microscopy, WSI review, and AIUC. In the second stage, performance metrics, including diagnostic accuracy, inter- and intra observer agreement, and screening time, were compared across methods. The results demonstrated that AIUC improved sensitivity and predictive values while significantly reducing screening time compared to conventional diagnostic approaches. Despite its potential to enhance bladder cancer diagnostics, further validation is needed for its integration into routine clinical practice.

In [17], a miRNA-based bladder cancer diagnostic model (MBCM) was provided to enhance diagnostic accuracy by integrating miRNA expression levels, demographic data, and routine laboratory test results. The MBCM framework consists of two stages: in the first stage, molecular biology techniques were applied to analyze urinary exosome miRNA expression, while clinical and demographic data were collected. In the second stage, three machine learning models Random Forest, SVM, and XGBoost were utilized to classify bladder cancer cases. The results demonstrated that combining miRNA data with patient clinical information improved performance, achieving an F1 score of 0.79 and an ROC of 0.85. Although MBCM showed promising potential as a non-invasive diagnostic tool, further validation is necessary to confirm its clinical applicability.

In [18], a cystoscopy-based bladder cancer detection model (CBCDM) was developed using HRNetV2, a semantic segmentation model, to identify tumor-related morphological features in white-light cystoscopy videos. The CBCDM framework was divided into two phases. The first involved manually annotating frames from a collection of recordings taken from patients having bladder tumors removed by transurethral resection or cystoscopy that had probable bladder lesions. In order to evaluate the model, the photos were divided into training and test sets and classified into groups with and without high and low resolution. The

results demonstrated that CBCDM effectively detected bladder lesions, with higher accuracy observed in high-resolution images compared to low-resolution ones. While the model showed strong diagnostic potential, further validation is necessary to ensure its reliability for clinical use

In [19], a histopathology-based bladder cancer subtyping model (HBCS) was introduced to classify basal and luminal subtypes of bladder cancer (BLCA) using deep learning features extracted from hematoxylin and eosin (H&E)-stained whole-slide images (WSIs). The HBCS framework consisted of two stages: in the first stage, WSIs from public databases and hospital cohorts were analyzed, and tumor patches were extracted using the RetCCL model. In the second stage, machine learning classifiers—support vector machine (SVM), random forest (RF), and logistic regression (LR) were trained on deep learning-derived features to differentiate between basal and luminal subtypes. The results demonstrated that the LR model, utilizing tumor patch features from the ResNet50 model, achieved superior performance, surpassing both junior and senior pathologists in subtype classification. While HBCS showed strong potential for improving molecular subtyping efficiency, further validation is required to ensure its clinical applicability.

In [20], a deep learning-based bladder cancer prediction model (DLBCP) was proposed to forecast the expression status of programmed cell death ligand 1 (PD-L1) using computed tomography (CT) imaging. The DLBCP framework consisted of two stages: in the first stage, convolutional neural networks and radiomics machine learning techniques were utilized to create prediction models based on imaging data from patients who underwent surgical removal of bladder cancer. In the second stage, the performance of the DL signature was compared with a radiomics-based model, and the optimal signature was integrated into a nomogram alongside clinical data. The internal decision-making process of DLBCP was further analyzed using Shapley additive explanation (SHAP) technology, revealing that tumor edge regions near the bladder wall had the most significant impact on predictions. While DLBCP demonstrated superior predictive performance and interpretability, further validation is required to confirm its clinical reliability.

Table 1: A comparison between the bladder cancer techniques.

Technique	Year of Publication	Advantages	Disadvantages	Accuracy
an immune-based prognostic learning model (IBPLM) [14]	• 2024	• **IBPLM** is Accurate Predicts response to ICI & chemotherapy	High computational cost; Needs clinical validation	88%
an AI-driven bladder cancer diagnosis model (AIBCM) [15]	• 2023	**AIBCM** Improves detection & classification; Enhances precision medicine	Requires large-scale validation	87%
an AI-assisted urinary cytology model (AIUC) [16]	• 2024	• **AIUC** Enhances diagnostic accuracy; Reduces screening time	Needs further validation	91%
A miRNA-based bladder cancer diagnostic model (MBCM) [17]	• 2025	• **MBCM is** Non-invasive; High accuracy	Requires further clinical validation	92%
A cystoscopy-based bladder cancer detection model (CBCDM) [18]	• 2025	• **CBCDM** is Effective in tumor detection	Lower accuracy in low-resolution images	94%
a histopathology-based bladder cancer subtyping model (HBCS) [19]	•2025	•**HBCS** is Accurate subtyping; Outperforms pathologists	Requires further validation	95%
a deep learning-based bladder cancer prediction model (DLBCP) [20]	• 2025	• HDLD Is High interpretability; Uses SHAP analysis	Needs clinical validation	94%
Bladder Cancer Diagnosis Strategy (BCDS)		• **BCDS** is an accurate method • Explainability • Robustness	• Its is Complexity • Not fast enough	97%

3. The proposed Bladder Cancer Diagnosis Strategy (BCDS)

The suggested Bladder Cancer Diagnosis Strategy (BCDS) will be covered in further detail in this section. Pre-Processing Phase (PP) and Bladder Cancer Diagnosing Phase (BDP) are the two successive steps that make up BCDS, as shown in Fig. 1. A set of pictures of bladder cancer provides the system's input.
The dataset is initially balanced and, if required, expanded during the PP phase. Following that, three important steps are carried out in order: feature extraction, feature selection and outlier rejection. A pre-trained deep learning model, such as GoogleNet [21], DenseNet [22], or AlexNet [23], is used to extract features from images. Then, using a bio-inspired optimization method called LSO, only the most informative features are kept once the extracted features have gone through the feature selection step. Lastly, using the IQR approach, the outlier rejection step removes errant or stray data points from the dataset [29].

The study uses AlexNet, GoogleNet, and DenseNet for feature extraction because to their complementing architectural properties. AlexNet establishes a core CNN structure; GoogleNet adds inception modules for multi-scale processing; and DenseNet enables feature reuse and fast training. These models were also chosen to strike a balance between performance and computing efficiency. Furthermore, to test the robustness of our model choices, we performed a comparison study using ResNet-50, which produced equivalent or slightly superior results at a greater computational cost.

On the other hand, in BDP, a recently suggested method that combines Grid Search cross-validation and KNN is used to actually diagnose bladder cancer. This method is utilized to determine the best way to set up the model's hyper parameters, including the number of neighbors (k) and the kind of distance measure, to get the best diagnostic accuracy. The model is refined to provide dependable and consistent performance in identifying bladder cancer patients based on clinical data inputs by methodically experimenting with different parameter combinations using Grid Search and testing them using cross-validation.

4.1 Feature extraction Phase (FEP) using deep learning pre-trained models.

The aim of the feature extraction procedure is to transform unstructured data into insightful representations that improve machine learning algorithms' performance. Pre-trained deep learning models like GoogleNet, DenseNet, and AlexNet have recently shown remarkable accuracy in identifying deep characteristics in input photos. Consequently, it is a potential strategy to choose one of these models for feature extraction in the suggested BCDS system. Subsection 5.6 will carry out a comparison study to determine the most efficient feature extractor in order to do this.

Using characteristics taken from each model separately, a typical classifier is trained for the comparison, and the model with the greatest classification accuracy is chosen. GoogleNet showed nearly human-level performance [30]. The Inception module is a crucial part of this deep network; GoogleNet uses nine Inception modules in all. GoogleNet focuses on the correlations between adjacent pixels in a picture. Modified versions of the Inception module serve as the foundation for GoogleNet and the other deep learning models in the Inception module.

There are two main versions of GoogleNet available to the public: Inception-ResNet and Inception versions 1 to 4. The Inception architecture replicates the ideal local sparse structure of visual networks using a "network within a network" approach. Before applying computationally expensive 3×3 or 5×5 convolutions, Inception utilizes more efficient 1×1 convolutions to perform dimensionality reduction. As datasets grow larger, computational power increases, and models become more advanced, the development of new algorithms and optimized network architectures plays a crucial role in enhancing recognition capabilities.

The second model is densely connected convolutional networks (DenseNet). DenseNet has achieved outstanding performance in image classification applications by tackling the vanishing gradient problem and enhancing feature propagation. The main feature of this deep network is its dense connection, which connects each layer directly to every other layer in a feed-forward fashion. This design optimizes information flow between layers and improves feature reuse, resulting in more efficient training. DenseNet decreases the amount of parameters in the network by enabling each layer to reuse features from previous levels, which is an effective method for improving model performance.

There are multiple versions of DenseNet available, including DenseNet-121, DenseNet-169, DenseNet-201, and DenseNet-264, each differing in depth and complexity. Unlike traditional deep networks that rely on isolated layers, DenseNet establishes direct connections between all layers, significantly reducing the number of parameters while maintaining high performance. Before applying complex transformations,

DenseNet leverages 1×1 convolutions for feature reduction and 3×3 convolutions for feature extraction. As datasets grow in size, and computational capabilities advance, the introduction of optimized architectures like DenseNet plays a crucial role in enhancing recognition accuracy while maintaining computational efficiency.

The third model is AlexNet was one of the pioneering deep learning models that revolutionized image classification by significantly outperforming traditional machine learning approaches. AlexNet played a major role in the rise of deep learning by demonstrating the power of convolutional networks at a large scale.The key component of this deep network is its deep convolutional architecture, consisting of eight layers five convolutional layers followed by three fully connected layers. AlexNet introduced innovations such as ReLU activation functions, overlapping max-pooling, and dropout regularization, which helped improve training efficiency and prevent overfitting.

There is a single standard version of AlexNet, which played a crucial role in the success of deep learning by winning the ImageNet Large Scale Visual Recognition Challenge (ILSVRC) in 2012. Unlike shallow networks, AlexNet utilizes large convolutional filters and deep feature extraction to improve classification accuracy. Before applying complex transformations, it employs max-pooling layers to reduce spatial dimensions and computational complexity. As datasets expand and computational power increases, architectures like AlexNet remain foundational in deep learning, paving the way for more advanced models with improved performance and efficiency.

4.2 Feature selection Phase (FSP) using bio-inspired optimization

The aim of feature selection is to pinpoint the exact characteristics in the dataset that are most helpful for the classification tasks based on a set of criteria, such as consistency, originality, and meaningfulness. Because it specifies the components that will be used to optimize efficiency, feature selection is the most important step in feature engineering. how many features are extracted throughout the deep learning process. LSO, a bioinspired optimizer. LSO is a straightforward swarm intelligence system that draws inspiration from the hunting techniques of leopard seals. it has been shown to outperform earlier swarm optimization methods in terms of speed and accuracy in identifying the optimal set of features at all search agent counts. LSO's high degree of flexibility allows it to solve real-time engineering challenges with speed and accuracy while avoiding local optima problems. Binary numbers (0 and 1) are utilized to confine the search space. Therefore, the meta-heuristic optimizers based on continuous values will have to be modified to handle the binary outputs corresponding to the selected features. To indicate whether a feature in the n-feature set will be considered in the classification process, it can be given a value of either 0 or 1.

4.3 **Outlier Rejection Phase (ORP)**

The majority of anomalies fall into one of two categories: (i) outliers and (ii) stray items. While the stray things are class-related but of little significance, the former are those that are thought to be irrelevant to the class. Since both kinds of anomalies have the potential to negatively impact the categorization decision, they must be removed during the preprocessing phase. Regretfully, the majority of classifications are made using the things that are located farthest from the class center. Therefore, incorrect categorization choices will undoubtedly be made if these things are the furthest away and represent invaders or have a weak degree of belonging to the class.

The interquartile range (IQR) will be used to identify and reject outliers in this section. It is well known that IQR quantifies the distribution and concentration of data. As a result, outliers' items that are situated far from the class center—can be effectively eliminated using it. IQR is resilient against outliers, in contrast to other outlier identification techniques where the computations are impacted by the outliers themselves.

Additionally, while using IQR, data is not compelled to adhere to any particular distribution, which makes it adaptable and efficient.

We first extract a numerical characteristic, such the average brightness, from each image before using IQR to image processing. Next, we determine the data's 25th and 75th percentiles, or the first quartile (QI1) and third quartile (QI3). The IQR is calculated as follows:

$$IQR = QI3 - QI1$$

This allows us to specify the range of values that are acceptable:

$$Lower\ Bound = QI1 - 1.5 \times IQR$$
$$Upper\ Bound = QI3 + 1.5 \times IQR$$

Images that have feature values outside of this range are rejected because they are deemed outliers

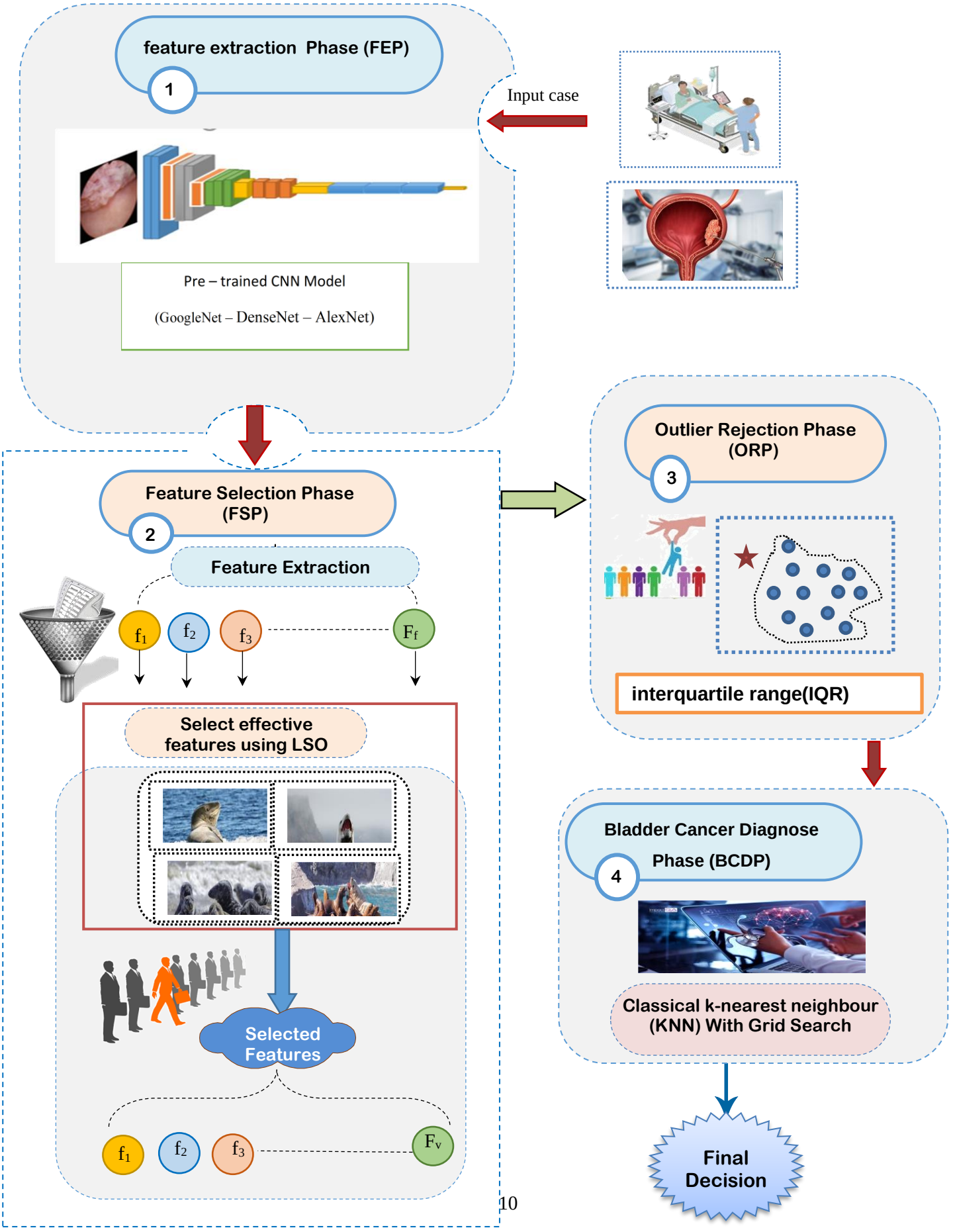

Fig 1 , The framework to diagnose bladder cancer .

4.4 Bladder Cancer Diagnose Phase (BCDP).

One popular machine learning classification method is the KNN algorithm, which classifies a data point according to the majority class of its closest neighbors. Selecting the appropriate hyper parameters, such as the distance metric and the number of neighbors (K), is crucial to KNN success. Manually choosing these criteria can be ineffective and result in less-than-ideal precision. Grid Search is utilized to methodically investigate various hyper parameter combinations in order to overcome this difficulty and identify the optimal setup that optimizes classification accuracy.

Data preparation is the first step in the process, during which the dataset is divided into training and testing sets. While the testing set is set aside for assessing the final optimized model, the training set is utilized to train the KNN models with various hyper parameter values. A variety of values for the number of neighbors ($K = \{3, 5, 7, 9, 11\}$) and several distance metrics are then specified on a parameter grid. The grid can additionally take into account the weight function, which determines whether each neighbor contributes equally or according to distance.

Grid Search with cross-validation is used after the grid parameter has been specified. The dataset is further divided into many training and validation subsets in this stage, and several KNN models are trained and evaluated on each subset. The Grid Search approach computes the accuracy for each conceivable combination of hyper parameters by methodically evaluating them. The combination with the highest validation accuracy, or the best performance, is chosen. Instead of only memorizing the training set, this guarantees that the model performs effectively when applied to new data.

A final KNN model is trained with the best settings and assessed on the test set once the ideal hyper parameters have been identified. This stage guarantees that the parameters chosen increase the categorization accuracy in the real world. Machine learning professionals may automate hyper parameter tweaking by utilizing Grid Search, which removes uncertainty and greatly enhances KNN's prediction capabilities. For real-world uses like fraud detection, recommendation systems, and illness diagnosis, this optimization procedure increases KNN's dependability.

4.4.1. Using K-Nearest Neighbors (KNN) and Grid Search for Bladder Cancer Diagnosis

In order to enhance patient outcomes, bladder cancer is a dangerous disorder that has to be detected early and accurately. KNN is one of the machine learning approaches that has been utilized more and more to help with medical diagnostics by examining patient data and finding patterns that suggest the presence of cancer. KNN classifies a new patient based on the most comparable patients by comparing their medical information, which is the output of previous stage (PP). So, choosing the appropriate hyper parameters, such as the number of neighbors (K) and the distance metric to gauge similarity, is crucial to KNN's accuracy.

Grid Search is used to tune these hyper parameters in order to improve the performance of KNN in the diagnosis of bladder cancer. Medical datasets are gathered and preprocessed, then divided into training and testing sets. Multiple values for K, distance metrics (such as Manhattan and Euclidean), and weighting techniques are systematically explored within a predetermined grid of hyper parameters. Grid Search with cross-validation evaluates several KNN models and determines the configuration that produces the best accuracy. Effective hyper parameter tuning lowers the possibility of misclassification, increasing correctly

recognized cancer cases and reducing false positives. This method improves KNN's dependability in helping physicians with early detection.

Although KNN is simple, accurate, and easy to implement, it is a lazy learner, and its performance is sensitive to the choice of k value, which may lead to misdiagnosis [29]. KNN uses a voting method to classify patients, which can be inaccurate. Therefore, it is essential to apply Grid Search on training data before classifying new patients. As shown in Fig. 2, DP begins by selecting patients in the testing dataset using Grid Search crossover as a weighting method. These weighted patients are then added to the training data for KNN classification.

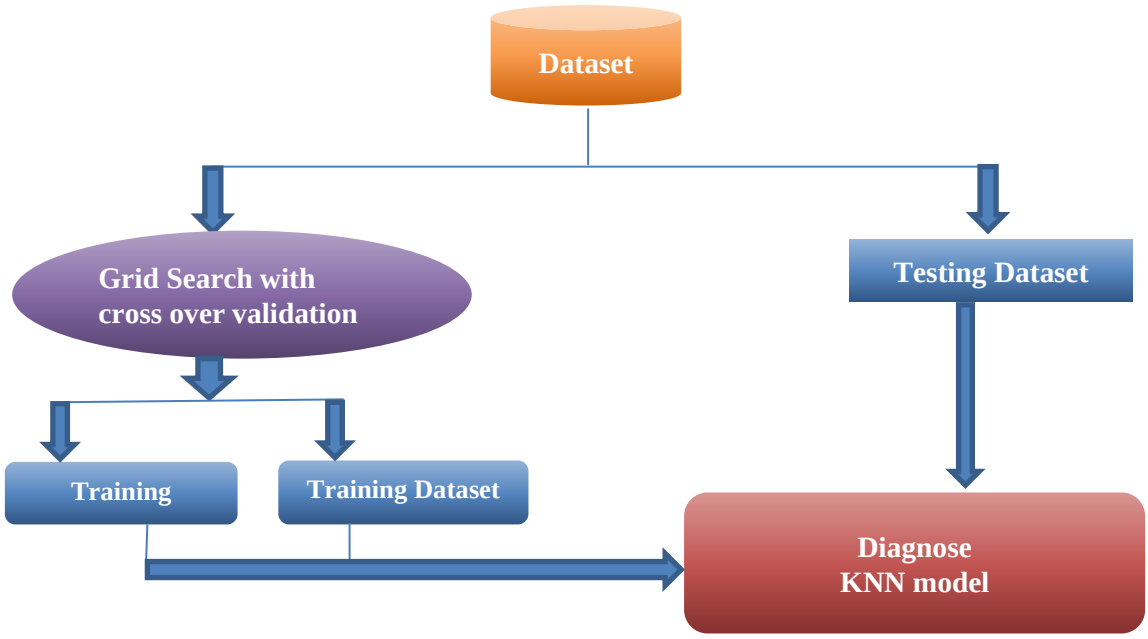

Fig 2, the steps of grid search and KNN model

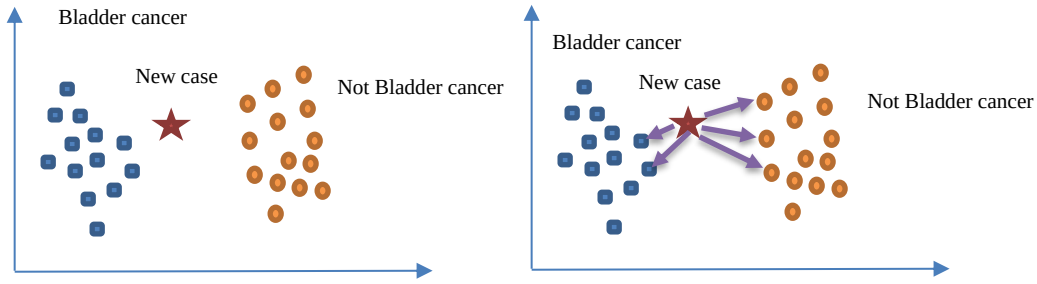

Fig 3, Diagnose bladder cancer use KNN

The K-nearest neighbors method is a member of the family of algorithms used in supervised learning. In theory, we want to understand the function h: X tends to Y so that, given an invisible observation x, With confidence, h(x) can forecast the matching output, y. When the distribution of incoming data is unknown, KNN is one of the most successful methods [31]. This method assigns a class to the query based on the majority labels of its k-nearest neighbors after determining the distance between the query and all of the training data. Because it performs well with large datasets and because the distribution of incoming current values may fluctuate over time, this method was selected for fault diagnosis. The performance of this

algorithm is strongly influenced by the settings of its hyper parameters [32].

The algorithm's output is greatly influenced by the following hyperparameters. Neighbors is For kneighbors queries, the default number of neighbors to utilize is Because it dictates how the points are handled, the weight function has a voice in predictions. For instance, nearer points may have more sway than farther points; the procedure is The nearest neighbors are calculated using a variety of procedures, and the metric is This option defines the distance metric that the algorithm will use to determine the distance. The operation of KNN is shown in these two pictures. Fig 3.

It is evident that the nearest neighbors rule classifies the red point as blue. Algorithm modifying is the last phase in the applied machine learning process before results are shown. It is frequently referred to as hyperparameter optimization, where the coefficients discovered by the machine learning algorithm itself are termed parameters and the algorithm parameters are called hyperparameters [33].The problem's search-nature is suggested by optimization. Finding an effective and reliable parameter, or collection of parameters, for an algorithm on a particular issue can be accomplished using a variety of search techniques. Grid Search CV is the one on which this study concentrates. Grid search is a parameter tuning technique that will systematically construct and assess a model for every set of algorithm parameters entered in a grid.

When applying Grid Search CV, it's important to understand the following terms: The scikit-learn estimator interface is implemented using Estimator.This parameter receives the classifier to be trained, and the parameter grid is a collection of parameter settings as values and parameter names as keys in a Python dictionary. To determine the greatest accuracy, every possible combination of these factors is examined. The cross validation splitting approach is decided by cross validation [34]. The process of resampling the available data in order to assess machine learning models is known as cross validation. The parameter K determines how many groups the provided data is divided into.This is mostly done to test how well machine learning models function on unknown data.

The primary benefit of this approach is that, in contrast to a straightforward train-test split, it produces fewer skewed or optimistic findings. The dataset is first randomly shuffled as part of the process. Next, k groups are created from the entire dataset. The test data is each group, and the training data is the other groups. The final summary is used to evaluate the model's performance once the evaluation ratings for each group are saved. Importantly, each sample is used k-1 times in training and only shows up once in the test data. The grid search cross validation procedure is clearly explained in Fig. 4.

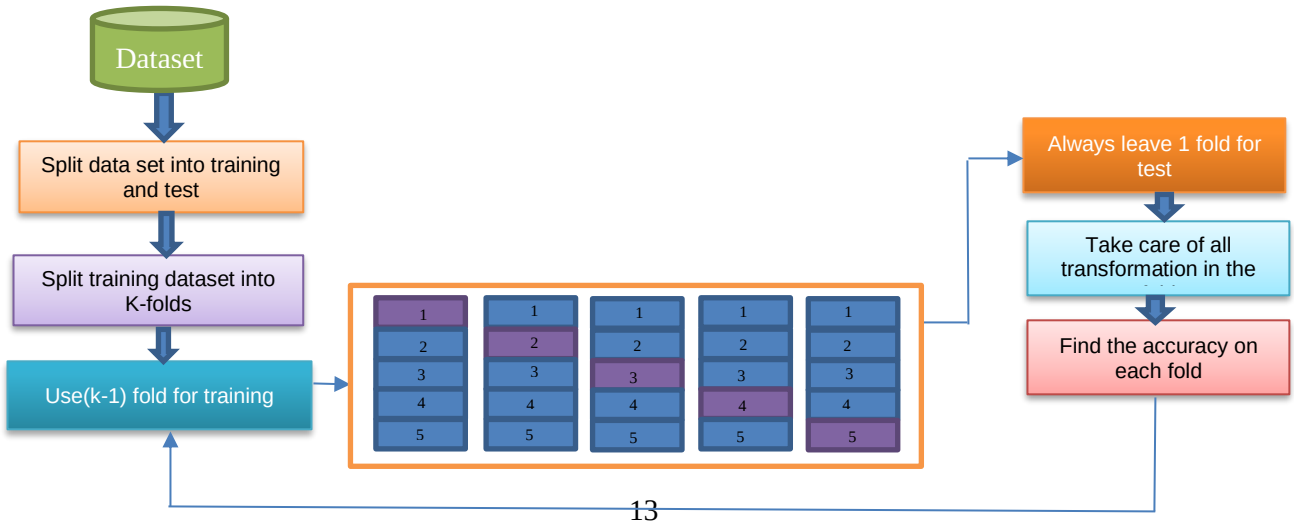

Fig 4, K fold cross validation

5 Simulation and Results.

In this section, the proposed **BCDS** that consists of two phases the first is pre-process (PP) and the second is (BDP) this model will be implemented against many modern diagnostic models to diagnose models to diagnose patients who suffer from bladder cancer. The evaluation scenario focuses on implementing and testing the **BCDS** against other recent strategies used for diagnosing bladder cancer. The primary objective is to validate the effectiveness of the **BCDS** in comparison to these approaches. The dataset used for this study is the Endoscopic Bladder Tissue dataset [24].

To demonstrate the accuracy and versatility of the **BCDS**, it is tested against various models using this dataset. The evaluation aims to show that **BCDS** can efficiently handle diverse data types and perform well on both large and small datasets. Performance metrics, including precision, accuracy, recall, and error rate calculated based on a confusion matrix are used to assess the models' effectiveness [25-26]. The models were deployed on an Nvidia GeForce GTX 1080 GPU and developed using TensorFlow 2.5 in Python 3.6. Each test in this study involved ten iterations of classifier training to ensure reliable results.

The classification task was performed using data obtained from pre-process (PP) phases. After conducting a series of evaluations with varying values of k, the value k = 6 was selected as the optimal parameter. This decision was based on the observation that further increases in k resulted in only marginal improvements in classification accuracy, while significantly increasing computational time. Therefore, k = 6 was identified as the most efficient trade-off between accuracy and processing cost. Also k for cross validation CV =10.

5.4 Performance metric

Confusion matrix metrics are automated evaluation methods used to classify false positives, false negatives, true negatives, and true positives, providing a comprehensive assessment of diagnostic performance. These metrics include accuracy, error rate, recall, precision, macro-average, micro-average, and F1-score [52, 53]. In this study, four primary evaluation metrics accuracy, recall, precision, and error rate are utilized to assess the proposed **BCDS** in two different scenarios. Additionally, macro-average, micro-average, and F1-score are incorporated to further evaluate the **BCDS**'s performance in comparison to other approaches. Table 2 presents the confusion matrix, while Table 3 provides the formulas used to compute these metrics.

Table 2: Confusion Matrix.

		Classified label	
		Positive	**Negative**
Known label	**Positive**	True Positive (TP)	False Negative (FN)
	Negative	False Positive (FP)	True Negative (TN)

Table 3: Confusion Matrix Formulas.

Metric	Formula	Meaning
Precision (P)	TP/(TP + FP)	The proportion of accurate positive forecasts.
Recall (R)	TP/(TP + FN)	The percentage of positive-labeled instances that were predicted to be positive.
Accuracy	(TP + TN) (TP + TN + FP + FN)	The proportion of accurate forecasts.
Error	1- Accuracy	The proportion of forecasts that are wrong.
Macro-average	$\sum_{i=1}^{c} p_i/c$ "for Precision"	The system's mean accuracy and recall for several categories.
	$\sum_{i=1}^{c} R_i/c$ "for Recall"	
Micro-average	(TP1 + TP2)/(TP1+ TP2 + FP1 + FP2) "for Precision"	The statistics are calculated by adding the total number of true positives, false positives, and false negatives for each class in the system.
	(TP1 + TP2)/(TP1 + TP2 + FN1 + FN2) "for Recall"	
F1-measure	2*PR/(P + R)	The precision and recall weighted harmonic mean.

5.5 Description of Bladder Cancer Dataset.

For this study, endoscopic videos and corresponding histological analyses from resected lesions were collected from 23 individuals undergoing TURBT [27]. With the guidance of a professional surgeon, the ocular data was matched with the histological results by analyzing the videos frame by frame. This process helped determine the specific bladder regions where lesions were removed during surgery. To eliminate ambiguity caused by multiple lesions of different types, only frames containing individual lesions were included in the dataset. This procedure was applied to each White Light Imaging (WLI) video.
There were four established categorization categories. In accordance with the World Health Organization's (WHO) and the International Society of Urological Pathology's (ISUP) general classification of bladder cancer [28], malignant tissue was classified into two groups: Low-Grade Cancer (LGC) and High-Grade Cancer (HGC). Furthermore, two additional classifications were taken into account for Non-Suspicious Tissue (NST) and No Tumor Lesion (NTL), the latter of which includes instances of cystitis brought on by inflammatory or infectious causes.

The dataset is broken out in depth in Table 4. The European Institute of Oncology (IEO) in Milan, Italy, is where the films were gathered. The study was approved by the IEO, and all patients gave their informed permission in compliance with the Helsinki Declaration. No private data was captured. There are 1,030 training photos, 151 testing images, and 245 validation images in the dataset.

Table 4: Composition pf the data set white light images.

Tissues types	No. of patient cases	No. of images for WLI
HGC	8	386
LGC	9	454
NST	5	439
NTL	5	97
total	23	1433

5.6 Evaluating Bladder Cancer Diagnosis Strategy (BCDS) Against Other Diagnoses models

In this section, the proposed BCDS is tested to evaluate its efficiency compared to other AI and deep learning diagnostic methods, namely IBPLM [14], AIBCM [15], AIUC [16], MBCM [17], and HBCS [19], as presented in Table 1. Figures (5–14) and Table 6 showcase the model's performance in terms of accuracy,

error rate, precision, recall, macro average, micro average, F1-score, and execution time. The results in Figure 23 and Table 6 indicate that the BCDS delivers highly accurate results with the shortest execution time compared to the other methods.

Table 5: The results of BCDS against other methods at the maximum number of training samples.

Prediction Methods	IBPLM	AIBCM	AIUC	MBCM	HBCS	BCDS
Accuracy	70	75	86	87	92	97
Error	30	25	14	13	8	3
Precision	87	92	93	92	92	94
Recall	89	90	91	91	92	95
F1-measure	90	92	91	92	94	96
Micro precision	90	91	92	93	94	94
Micro recall	88	89	92	93	93	94
Macro precision	90	92	93	94	95	96
Macro recall	89	90	92	93	92	95
Execution time	7.5	7	7.2	6.9	6.5	5.5
Execution time (s)	7.5	7	7.2	6.9	6.5	5.5

Figures 5 to 10 and Table 5 demonstrate that BCDS achieves the highest accuracy, precision, recall, and F1-score, while also recording the lowest error and execution time compared to other models, especially when using the maximum number of training samples.

Figures (5→10) and table 5 demonstrate that BCDS achieves the highest accuracy, precision, recall, and F1-score, while also recording the lowest error and execution time compared to other models, especially when using the maximum number of training samples. Related to figure 5 and table 5, the accuracy of IBPLM, AIBCM , AIUC , MBCM , HBCS and BCDS are 70%, 75%, 86%, 87%, 92%, and 97% respectively at the maximum number of training samples. Figure 6 and table 5 show that the error of IBPLM, AIBCM , AIUC , MBCM , HBCS and BCDS are 30%, 25% ,14% ,13%, 8% and 3% respectively. Figure 7 and table 5 show that the precision of IBPLM, AIBCM , AIUC , MBCM , HBCS and BCDS are 87%, 92% ,93% ,92% ,92% and 94% respectively. According to figure 8 and table 5, the recall of IBPLM, AIBCM , AIUC , MBCM , HBCS and BCDS are 89%, 90%, 91%, 91%, 92% and 95% respectively at the maximum number of training samples. According to figure 9 and table 5, F1-measures of IBPLM, AIBCM , AIUC , MBCM , HBCS and BCDS are 90%, 92%, 91%, 92%, 94% and 96% respectively at the maximum number of training samples. According to figure 23 and table 6, the maximum execution time is provided by IBPLM, AIBCM , AIUC , MBCM and HBCS but BCDS gives the minimum execution time at the maximum training sample number. The execution time of IBPLM, AIBCM , AIUC , MBCM , HBCS and BCDS are 7.5s, 7s, 7.2s, 6.9s, 6.5 and 5.5 respectively.

Figures (11→14) and table 6 show that the performance of micro precision, micro recall, macro precision, and macro recall are increasing according to the number of training samples. According to the maximum number of training samples, figure 11, figure 12 and table 5 show that IBPLM introduces 90% and 88% for micro precision and micro recall respectively. Additionally, AIBCM introduces 91% and 89% for micro precision and micro recall respectively. AIUC introduces 92% and 92% for micro precision, micro recall respectively. MBCM introduces 93% and 93% for micro precision and micro recall respectively. HBCS introduces 94% and 93% for micro precision and micro recall respectively. BCDS introduces 94% and 94% for micro precision and micro recall respectively. Thus, BCDS outperforms other models according to micro precision and micro recall.

From figure 13, figure 14 and table 5, IBPLM presents 90% and 89% for macro precision and macro recall respectively at the maximum number of training samples. AIBCM presents 92% and 90% for macro precision and macro recall respectively at the maximum number of training samples. AIUC presents 93%

and 92% while MBCM presents 94% and 93% for macro precision and macro recall respectively at the maximum number of training samples. HBCS presents 95% and 92% for macro precision and macro recall respectively at the maximum number of training samples. Finally, EDL presents 96% and 95% for macro precision and macro Recall respectively at the maximum training sample number.

In summary, the findings shown in Figures 5–10 and Table 5 clearly illustrate the superiority of the BCDS model over other models such as IBPLM, AIBCM, AIUC, MBCM, and HBCS. Specifically, BCDS gets the greatest accuracy, precision, recall, F1-score, as well as the lowest error rate and execution time, especially when the maximum amount of training samples are used. For example, with the maximum amount of training samples, BCDS achieves an accuracy of 97%, greatly surpassing other models such as IBPLM (70%), AIBCM (75%), and AIUC (86%). Furthermore, BCDS has the lowest error rate (3%) and the shortest execution time (5.5 seconds), demonstrating its efficiency. Furthermore, BCDS excels in micro and macro accuracy and recall, demonstrating consistently good performance across several assessment parameters. These findings demonstrate that BCDS is not only more accurate, but also faster and more efficient in identifying bladder cancer than other examined models. According to these findings, BCDS has outstanding potential for usage in real-world applications, providing accurate and quick diagnoses.

In this section, the optimal feature extractor is determined, The adopted methodology involves utilizing multiple pre-trained Convolutional Neural Network (CNN) architectures to extract deep features from a defined set of training images. The extracted features are structured into a tabular dataset, which is subsequently employed to train conventional machine learning classifiers independently for each CNN model. Each trained classifier is then evaluated using a separate test image dataset to assess its diagnostic performance in terms of accuracy. The CNN architectures selected for comparison due to their proven effectiveness and extensive adoption in the literature are VGG16, AlexNet, and GoogleNet. As illustrated in Fig. 15 and detailed in Table 6, the average classification accuracy obtained from each feature extractor indicates that GoogleNet provides the highest performance, and thus is selected as the feature extractor for the proposed BCDS framework.

In response to reviewer comments, we ran an extra experiment to compare the performance of our chosen models (AlexNet, GoogleNet, and DenseNet) against a more contemporary design, ResNet-50. Using the same dataset and assessment measures, ResNet-50 achieved an accuracy of 86%.in table 6. ResNet-50 marginally beat AlexNet and GoogleNet in terms of accuracy, but it performed similarly to DenseNet at a substantially larger computational cost. These data show that the models we selected offer a competitive trade-off between performance and efficiency. Future work will include further study with topologies such as EfficientNet.

Table 6: "Comparison of the selected feature extraction models with respect to their average diagnostic accuracy."

Model	Accuracy
GoogleNet	87%
DenseNet	75%
AlexNet	69%
ResNet-50	86%

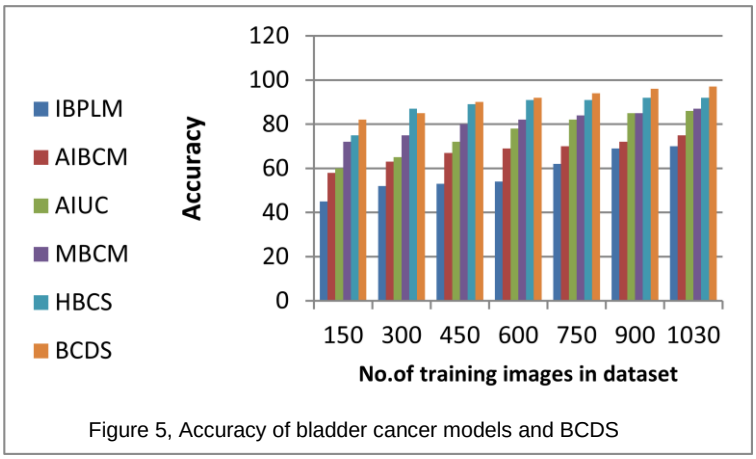

Figure 5, Accuracy of bladder cancer models and BCDS

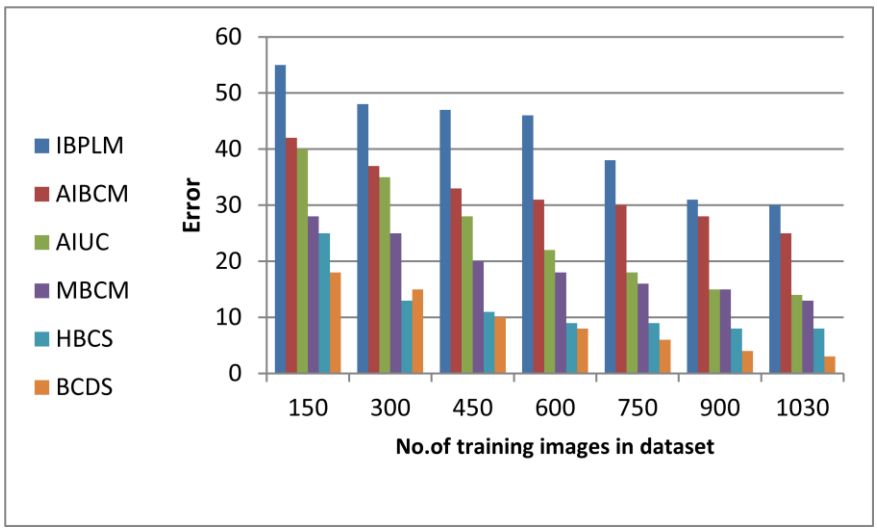

Figure 6, Error of bladder cancer models and BCDS

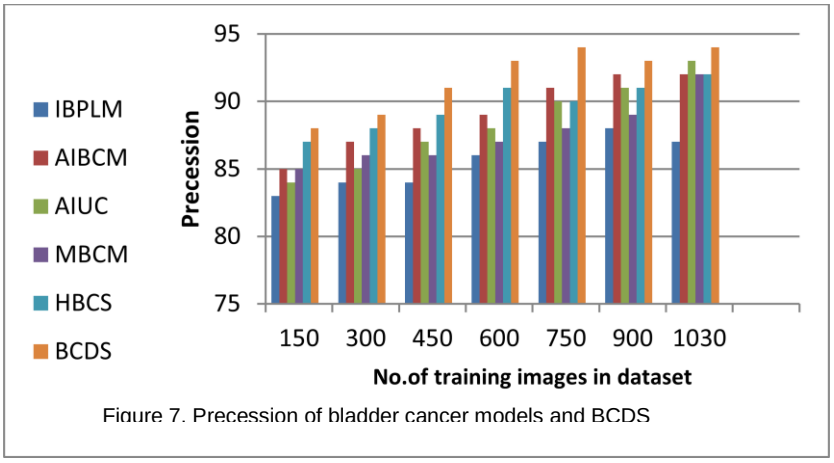

Figure 7. Precession of bladder cancer models and BCDS

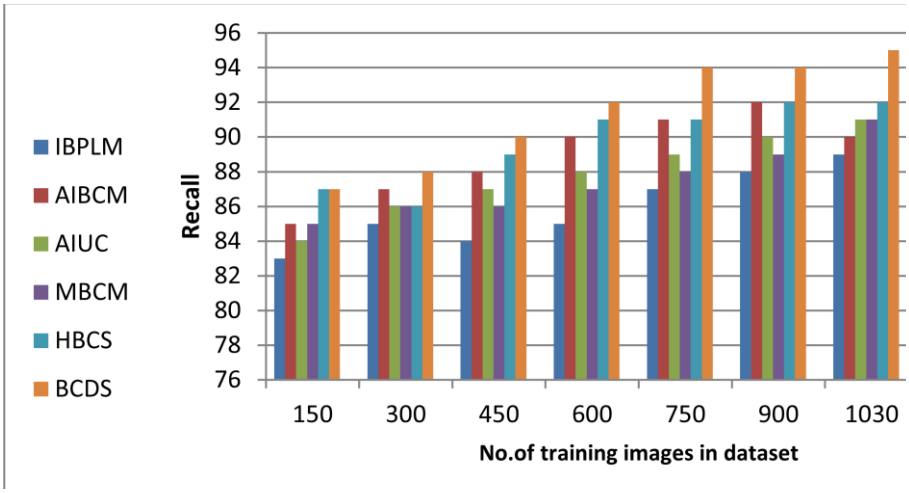

Figure 8, Recall of bladder cancer models and BCDS

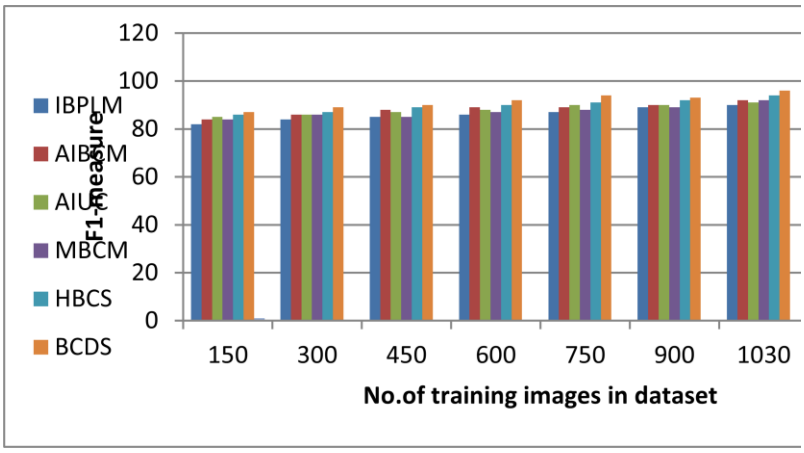

Figure 9, F1- measure of bladder cancer models and BCDS

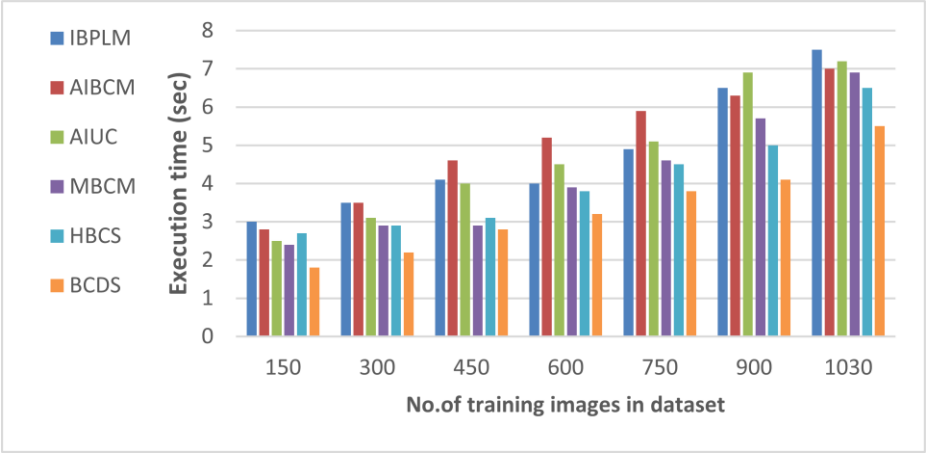

Figure 10, Execution time of bladder cancer models and BCDS

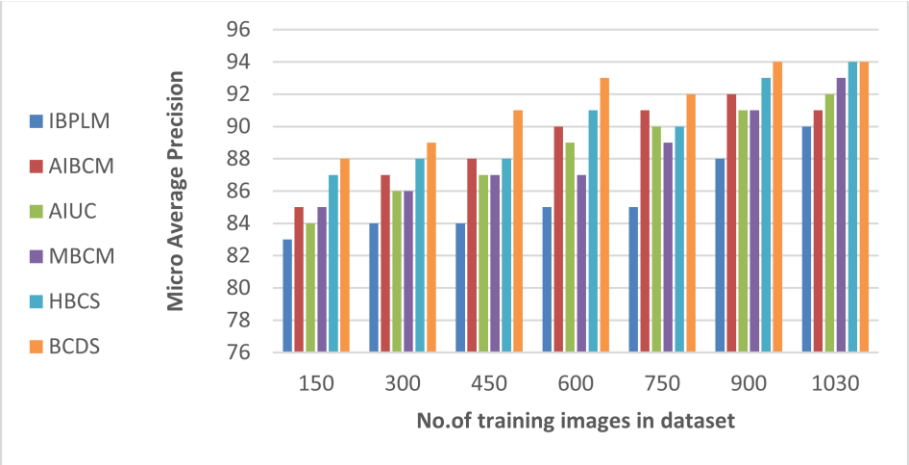

Figure 11, Micro Average Precision of bladder cancer models and BCDS

Figure 12, Micro Average Recall of bladder cancer models and BCDS

Figure 13, Macro Average Precision of bladder cancer models and BCDS

Figure 14, Macro Average Recall of bladder cancer models and BCDS

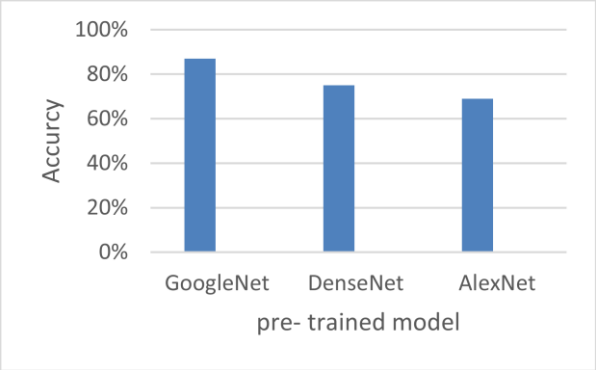

Figure 15, Accuracy of different pre-trained CNN models

6 **Conclusions and Future Works**

The Bladder Cancer Diagnosis Strategy (BCDS) effectively combines image processing and machine learning methods to increase the diagnosis accuracy of bladder cancer. It is divided into two main stages: the Bladder Cancer Diagnosis Phase (BDP) and the Pre-Processing Phase (PP). Following dataset balancing and any necessary augmentation, the PP phase involves feature extraction utilizing models like GoogleNet, DenseNet, and AlexNet, and feature selection using Leopard Seal Optimization (LSO). Using Grid Search cross-validation, the BDP phase optimizes the K-Nearest Neighbors (KNN) classifier's hyper parameters for precise diagnosis. The outcomes demonstrate how well the model can identify bladder cancer and provide encouraging diagnostic reliability. Future research will concentrate on adding more varied imaging modalities to the dataset and incorporating further diagnostic data, such as genetic information. Another area that needs work is real-time diagnostic capabilities, which would allow for quicker processing during patient screens. Performance might potentially be improved by investigating more sophisticated optimization techniques like particle swarm optimization or genetic algorithms. Additionally, enhancing the accuracy and resilience of the model would require clinical validation in real-world contexts and the possible incorporation of sophisticated models like Transformers or Capsule Networks.

References:

[1] R. L. Siegel, K. D. Miller, A. Jemal, “Cancer statistics, 2022”, Wiley, CA: A Cancer Journal for Clinicians, vol. 72, no. 1, 2022, pp. 7–33.

[2] American Cancer Society, “Bladder Cancer: Early Detection, Diagnosis, and Staging”, 2022. Retrieved from www.cancer.org

[3] P. Gontero, A. Birtle, O. Capoun, et al., “EAU guidelines on non–muscle-invasive urothelial carcinoma of the bladder”, Elsevier, European Urology, vol. 86, no. 6, 2024, pp. 531–549.

[4] A. Esteva, A. Robicquet, et al., “A guide to deep learning in healthcare”, Nature Publishing Group, Nature Medicine, vol. 25, no. 1, 2019, pp. 24–29.

[5] K. H. u, A. L. Beam, I. S. Kohane, “Artificial intelligence in healthcare”, Nature Publishing Group, Nature Biomedical Engineering, vol. 2, no. 10, 2018, pp. 719–731.

[6] S. Gulati, P. C. Patel, et al., “Machine learning applications in bladder cancer detection and treatment”, Journal of Urology Research, vol. 15, no. 3, 2021, pp. 205–219.

[7] R. Kumar, R. Srivastava, S. Srivastava, “A machine learning approach for bladder cancer prediction using KNN and decision tree algorithms”, Biomedical Signal Processing and Control, vol. 60, 2020, pp. 101992.

[8] H. Chen, Y. Shen, Q. Qin, X. Ni, Y. Zhang, J. Liu, et al., “Recent advances and clinical applications of deep learning in medical image analysis”, Elsevier, Medical Image Analysis, vol. 90, 2024, pp. 102155.

[9] A. H. Rabie, N. A. Mansour, A. I. Saleh, “Leopard seal optimization (LSO): A natural inspired meta-heuristic algorithm”, Communications in Nonlinear Science and Numerical Simulation, vol. 125, 2023, p. 107338

[10] N. Patel, K. Gaitonde, P. L. Choyke, □Artificial intelligence in bladder cancer imaging: Current status and future directions□, Nature Publishing Group, Scientific Reports, vol. 12, no. 1, 2022, pp. 22797.

[11] J. Lee, H. Kim, S. Park, □Deep learning-based cystoscopic image analysis for bladder cancer detection□, Frontiers Media, Frontiers in Oncology, vol. 14, 2024, pp. 1487676.

[12] R. Smith, A. Jones, T. Brown, □Machine learning applications in bladder cancer histopathology: A review of current advancements and challenges□, BMC, BMC Cancer, vol. 25, no. 1, 2025, pp. 13688.

[13] https://gco.iarc.who.int/today/en/dataviz/maps-heatmap?mode=population&types=1

[14] W. Nie, Y. Jiang, L. Yao, X. Zhu, A. Y. Al-Danakh, W. Liu, Q. Chen, D. Yang, “Prediction of bladder cancer prognosis and immune microenvironment assessment using machine learning and deep learning models”, Heliyon, vol. 10, no. 1, 2024, PP.1-19.

[15] G. Rossin, F. Zorzi, L. Ongaro, A. Piasentin, F. Vedovo, G. Liguori, A. Zucchi, et al., “Artificial Intelligence in Bladder Cancer Diagnosis: Current Applications and Future Perspectives”, Journal of

Clinical Medicine, vol. 11, no. 7, 2022, pp. 2030.

[16] T.-J. Liu, W.-C. Yang, S.-M. Huang, W.-L. Yang, H.-J. Wu, H. W. Ho, S.-W. Hsu, C.-H. Yeh, M.-Y. Lin, Y.-T. Hwang, P.-Y. Chu, "Evaluating artificial intelligence–enhanced digital urine cytology for bladder cancer diagnosis", Wiley, Cancer Cytopathology , vol. 132, no. 8, 2024, pp. 686–695.

[17] Ē. Bitiņa-Barlote, D. Bļizņuks, S. Silina, M. Šatcs, E. Vjaters, V. Lietuvietis, M. Nakazawa-Miklaševiča, J. Plonis, E. Miklaševičs, Z. Daneberga, J. Gardovskis, "Liquid Biopsy Based Bladder Cancer Diagnostic by Machine Learning", Diagnostics, vol. 15, no. 4, 2025, p. 492.

[18] Z. Ye, Y. Li, Y. Sun, C. He, G. He, Z. Ji, "Leveraging Deep Learning in Real-Time Intelligent Bladder Tumor Detection During Cystoscopy: A Diagnostic Study", Annals of Surgical Oncology, vol. 32, no. 5, 2025, pp. 1234–1242.

[19] Z. Zheng, F. Dai, J. Liu, Y. Zhang, Z. Wang, B. Wang, X. Qiu, "Pathology-based deep learning features for predicting basal and luminal subtypes in bladder cancer", BMC Cancer, vol. 25, no. 1, 2025, p. 13688.

[20] X. Han, J. Guan, L. Guo, Q. Jiao, K. Wang, F. Hou, S. Liu, S. Yang, C. Huang, W. Cong, H. Wang, "CT-based interpretable deep learning signature for predicting PD-L1 expression in bladder cancer: a two-center study", Cancer Imaging, vol. 25, no. 1, 2025, p. 27.

[21] J. Tan, Q. Le, "EfficientNetV2: Smaller models and faster training", Proceedings of the International Conference on Machine Learning (ICML), 2021, pp. 10096–10106.

[22] Z. Liu, H. Mao, C. Wu, C. Feichtenhofer, T. Darrell, S. Xie, "A ConvNet for the 2020s", Proceedings of the IEEE/CVF Conference on Computer Vision and Pattern Recognition, 2022, pp. 11976–11986.

[23] A. Dosovitskiy, L. Beyer, A. Kolesnikov, D. Weissenborn, X. Zhai, T. Unterthiner, et al., "An image is worth 16x16 words: Transformers for image recognition at scale", Advances in Neural Information Processing Systems, vol. 33, 2020, pp. 11900–11912.

[24] S. Fouladi, A. Safaei, N. Arshad, M. Ebadi, A. Ahmadian, "The use of artificial neural networks to diagnose Alzheimer's disease from brain images", Springer, vol. 81, Aug 2022, pp. 37681–37721.

[25] A. Rabie, A. Saleh, N. Mansour, "A Covid-19's integrated herd immunity (CIHI) based on classifying people vulnerability," Elsevier, vol. 140, 2022, pp. 1–29.

[26] A. Rabie, N. Mansour, A. Saleh, et al., "Expecting individuals' body reaction to Covid-19 based on statistical Naïve Bayes technique," Elsevier, vol. 128, 2022, pp. 1–23.

[27] Z. Liu, Y. Lin, Y. Cao, H. Hu, Y. Wei, Z. Zhang, S. Lin, B. Guo, "Swin Transformer: Hierarchical vision transformer using shifted windows", Proceedings of the IEEE/CVF International Conference on Computer Vision (ICCV), 2021, pp. 10012–10022.

[28] O. Sanli et al., "Bladder cancer," Nature Rev. Dis. Primers, vol. 3, no. 1, 2017, pp. 1–19.

[29] A. I. Saleh, S. A. Hussien, "Monkeypox diagnosis based on probabilistic K-nearest neighbors

(PKNN) algorithm", Computers in Biology and Medicine, vol. 186, 2025.

[30] C. Szegedy, W. Liu, Y. Jia, P. Sermanet, S. Reed, D. Anguelov, D. Erhan, V. Vanhoucke, and A. Rabinovich, "Going deeper with convolutions," *Proceedings of the IEEE Conference on Computer Vision and Pattern Recognition (CVPR)*, 2015, pp. 1-9.

[31] Halder, R. K., Uddin, M. N., Uddin, M. A., Aryal, S., & Khraisat, A. (2024). "Enhancing K-nearest neighbor algorithm: a comprehensive review and performance analysis of modifications." *Journal of Big Data, 11*, 113.

[32] Daulay, R. S. A., Efendi, S., & Suherman. (2023). "Review of Literature on Improving the KNN Algorithm." *Transactions on Engineering and Computing Sciences, 11*(3), 63–72.

[33] Vahedifar, M. A., Akhtarshenas, A., Sabbaghian, M., Rafatpanah, M. M., & Toosi, R. (2023**).** "Information Modified K-Nearest Neighbor."

[34] Vahedifar, M. A., Akhtarshenas, A., Sabbaghian, M., Rafatpanah, M. M., & Toosi, R. (2023). "Information Modified K-Nearest Neighbor."